

# Syntheses and remarkable photophysical properties of 5-(2-pyridyl)pyrazolate boron complexes; photoinduced electron transfer†

Chung-Chih Cheng,<sup>a</sup> Wei-Shan Yu,<sup>b</sup> Pi-Tai Chou,<sup>\*b</sup> Shie-Ming Peng,<sup>b</sup> Gene-Hsiang Lee,<sup>b</sup> Pei-Chi Wu,<sup>c</sup> Yi-Hwa Song<sup>c</sup> and Yun Chi<sup>\*c</sup>

<sup>a</sup> Department of Chemistry, Fu-Jen Catholic University, 242, Shin Chuang, Taiwan, ROC

<sup>b</sup> Department of Chemistry, National Taiwan University, 106, Taipei, Taiwan, ROC

<sup>c</sup> Department of Chemistry, National Tsing Hua University, 300, Hsinchu, Taiwan, ROC.

E-mail: chop@ccms.ntu.edu.tw; ychi@mx.nthu.edu.tw

Received (in Cambridge, UK) 5th August 2003, Accepted 28th August 2003

First published as an Advance Article on the web 12th September 2003

A new series of pyridyl pyrazolate boron complexes **2a–e** have been synthesized, in which **2a–c** exhibit remarkable dual fluorescence properties due to the photoinduced electron transfer reaction.

Boron complexes with conjugated light-emitting  $\pi$ -systems have recently received considerable attention due to their potential uses in organic light emitting devices (OLED)<sup>1</sup> as well as biomolecular probes.<sup>2</sup> It has been a core interest to chemically modify the ligand chromophores so that the physical properties can be fine-tuned to achieve a designated function. In this communication, we report the syntheses and photophysical studies of a new series of 5-(2-pyridyl) pyrazolate boron complexes. 5-(2-Pyridyl) pyrazole was selected because it can function as a chelating ligand upon treatment with a boron compound such as BPh<sub>3</sub>, giving a nearly planar, conjugated  $\pi$ -system that was perfect for studying the photoluminescent properties.

Pathways leading to the synthesis of 5-(2-pyridyl) pyrazolate boron complexes are shown in Scheme 1. The required 2'-(2-pyridyl) pyrazoles (**1a–e**) were first synthesized using methods reported in the literature.<sup>3</sup> Subsequently, treatment of **1a–e** with BPh<sub>3</sub> in THF solution affords the target BPh<sub>2</sub> complexes **2a–e** in good yields of  $\geq 87\%$ . Similar treatment of **1a** with B(C<sub>6</sub>F<sub>5</sub>)<sub>3</sub>, followed by recrystallization from a solution of CH<sub>2</sub>Cl<sub>2</sub> and methanol, affords a colorless crystalline solid **2f** in 48% yield.

A typical crystal structure of **2a** is depicted in Fig. 1, along with the selected metric parameters. It is notable that the boron atom has a characteristic tetrahedral geometry with angles N(1)–B(1)–N(2) = 93.43(13)° and C(10)–B(1)–C(16) = 117.30(15)°. The 5-(2-pyridyl) pyrazolate ligand is chelated to the boron atom with bond distances, B(1)–N(1) = 1.629(2) Å and B(1)–N(2) = 1.570(2) Å, for which the N(1)–B dative distance is found to be distinctively longer than that of the N(2)–B distance. This observation is consistent with the structural

data reported in other tetrahedrally arranged BPh<sub>2</sub> complexes with chelating ligands of (2-pyridyl)-7-azaindole and (2-pyridyl)-7-indole derivatives.<sup>4</sup> Moreover, the phenyl rings are orthogonal to the 5-(2-pyridyl)pyrazolate ligand, which is confirmed by the observation of two nearly perpendicular dihedral angles of 73.9°–77.1°. Their overall molecular structure resembles that of the 9,9-disubstituted fluorene compounds, which have been widely used as the most promising blue-phosphor in OLED applications.<sup>5</sup>

As listed in Table 1 the S<sub>0</sub> → S<sub>1</sub> ( $\pi\pi^*$ ) absorption spectral features of **2a–e** ( $\lambda_{\text{max}} \sim 315\text{--}350$  nm) in THF reveal bathochromic shifts with respect to their free ligands **1a–e** ( $\lambda_{\text{max}} \sim 290\text{--}300$  nm). The  $\pi\text{--}\pi^*$  transition of **2a–e** is principally localized on the planar pyridyl pyrazolate ligands, on which the HOMOs and LUMOs are mainly located at the pyrazolate and the pyridyl sites, respectively. The B–N covalent interaction is believed to exist at the pyrazolate side of the ligand, while the other N→B dative bonding resides at the opposite, pyridyl moiety. It is thus anticipated that the electron-deficient BPh<sub>2</sub> substituent would exert large stabilization on the pyridyl  $\pi$ -system due to its electron accepting capability with respect to

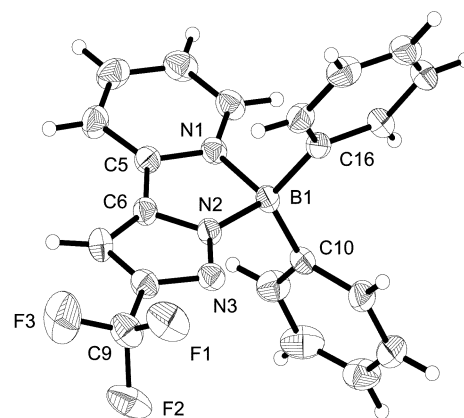
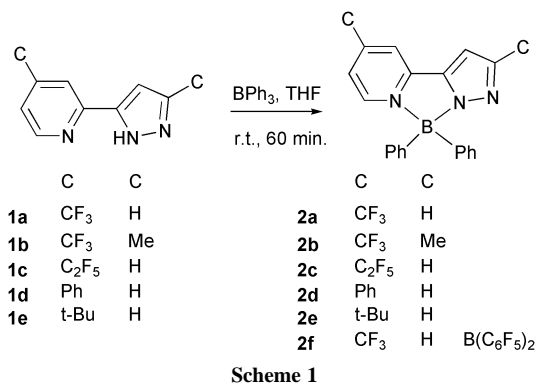


**Fig. 1** The X-ray crystal structure of **2a**; selected bond distances: B1–N1 = 1.629(2), B1–N2 = 1.570(2), B1–C10 = 1.596(3), B1–C16 = 1.609(3), N1–C5 = 1.352(2), N2–C6 = 1.336(2), N2–N3 = 1.336(2) Å.

**Table 1** Photophysical properties of **2** in THF (298K).

Solvent	$\lambda_{\text{max}}/\text{nm}^a$	PL $\lambda_{\text{max}}/\text{nm}$	$\tau/\text{ns}^b$ F <sub>1</sub>	$\tau/\text{ns}^b$ F <sub>2</sub>	E <sub>a</sub> <sup>c</sup> (kcal/mol)
THF					
<b>2a</b>	320	375, 505	0.53	(0.52*, 18.3)	1.31
<b>2b</b>	315	365, 488	0.42	(0.38*, 14.9)	1.16
<b>2c</b>	320	374, 512	0.50	(0.48*, 11.5)	1.10
<b>2d</b>	350	460	16.4	–	–
<b>2e</b>	340	430	9.9	–	–
<b>2f</b>	325	382	6.8	–	–

<sup>a</sup> Data was taken from the first vibronic peak. <sup>b</sup> Samples were degassed via three freeze-pump-thaw cycles. <sup>c</sup> obtained from the temperature dependent study in 2MTHF. \* denotes the rise time



† Electronic supplementary information (ESI) available: Photophysical experimental details, the spectral data of all boron complexes, and crystal data of **2a**. See <http://www.rsc.org/suppdata/cc/b3/b309374c/>

that of the covalent characteristics of the pyrazolate fragment, resulting in significant red-shift from the corresponding **1a–e** ligands.

**2d** and **2e** exhibited strong, single fluorescence maximized at 460 and 430 nm, respectively in THF (see Fig. 2 for **2e**). Similar results were observed in the solid crystal. Conversely, while the solid crystal of **2a–c** showed only one emission centered at 382, 360 and 370 nm, respectively, dual emission was observed in solution, consisting of a normal emission band (**2a**: 375, **2b**: 365 and **2c**: 374 nm, the F<sub>1</sub> band) and an anomalously large Stokes shifted emission (**2a**: 505, **2b**: 488 and **2c**: 512 nm, the F<sub>2</sub> band) in THF. The excitation spectra for both F<sub>1</sub> and F<sub>2</sub> bands are identical, which are also effectively the same as the absorption profile, excluding its origin from traces of impurity. In contrast to the nearly solvent independent F<sub>1</sub> emission frequency, the fluorescence peak frequency for the F<sub>2</sub> band was linearly proportional to solvent polarity ( $\Delta f$ ).<sup>†</sup> Accordingly, a change of dipole moment of  $\sim 6.6$  Debye between ground and excited states was deduced.

Further insight into the correlation of dual emission properties was gained from the dynamic studies. As shown in Table 1 the lifetime of the F<sub>1</sub> band for **2a** was fitted to be  $\sim 0.53$  ns ( $\chi^2 = 1.02$ ) at 298 K, while the F<sub>2</sub> band is apparently composed of rise and decay components that were fitted to be 0.52 ns and 18.3 ns, respectively ( $\chi^2 = 1.05$ ). The rise time of the F<sub>2</sub> band, within experimental error, is identical with the decay time of the F<sub>1</sub> band, supporting a precursor-successor type of relaxation mechanism. As shown in Fig. 3, the F<sub>1</sub>/F<sub>2</sub> ratio for **2a** increased upon decreasing the temperature. The reaction rate monitored by the decay dynamics of the F<sub>1</sub> band or equivalently the rise dynamics of the F<sub>2</sub> band revealed significant temperature dependence (see insert of Fig. 3). Similar dual emission and precursor-successor related dynamics were also obtained for **2b** and **2c** and the results are listed in Table 1.

The above results can plausibly be rationalized by a mechanism incorporating a photoinduced electron transfer (ET) process from the phenyl moiety to the pyrazolate ligand. The separations from the center of two phenyl fragments to the center of pyridyl and pyrazolate ring systems are estimated to be 4.6–4.7 Å and 4.9–5.0 Å, respectively. These lengths are significantly shorter than the typical distance ( $\sim 7$  Å) that allows the occurrence of through-space electron transfer. The reduction peak potential of 5-(2-pyridyl) pyrazolate complexes **2a–b** and **2d–e** occurred at  $-1.67$ ,  $-1.72$ ,  $-1.76$  and  $-1.86$  V, respectively in CH<sub>3</sub>CN. The decrease of reduction potential correlates well with the trend of electron withdrawing properties of substituents at the pyrazolate ligand. The result, in combination with the increase of the absorption energy gap being in the order of **2a**  $\sim$  **2b**  $\sim$  **2c**  $>$  **2d**, **2e**, qualitatively rationalizes the occurrence of ET in **2a–c**. To further support for the phenyl ring acting as an electron donor in the proposed ET mechanism we also synthesized **2f** in which the absorption gap is similar to **2a**, whereas the phenyl ring is replaced by a perfluorophenyl moiety

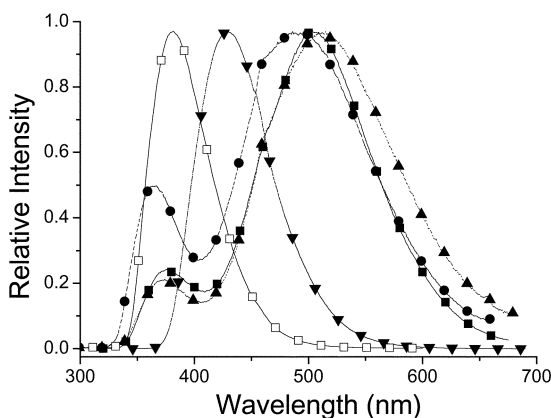


**Fig. 2** Emission spectra of (a) **2a** (■), (b) **2b** (●), (c) **2c** (▲), (d) **2e** (▼) and (e) **2f** (□) in THF.

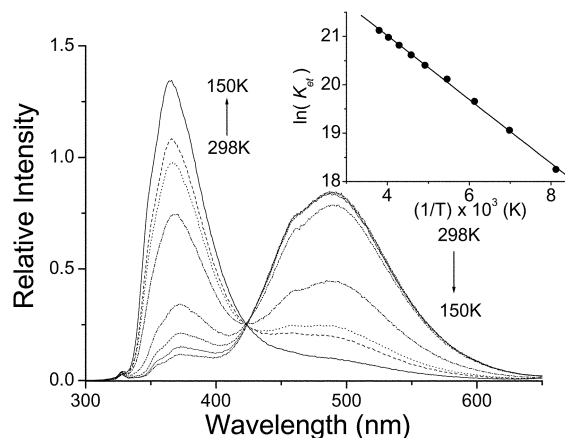


**Fig. 3** Temperature-dependent emission spectra of **2a** in 2MTHF at 298–150 K. Insert: The plot for  $\ln(k_{\text{obs}})$  versus the reciprocal of temperatures.

to increase the relative oxidation potential. As a result, ET process is prohibited in **2f**, as indicated by a unique, normal emission band maximum at 382 nm (see Fig. 2).

The drastic difference in photophysics between single crystal (single, normal emission) and solution phase (dual emission) in **2a–c** is intriguing. The logarithm plot of the ET rate<sup>6</sup> vs.  $1/T$  is sufficiently linear (insert of Fig. 3), from which a barrier of 1.31 kcal mol<sup>-1</sup> and a frequency factor of  $1.88 \times 10^{10}$  s<sup>-1</sup> were deduced for **2a**. The  $E_a$  value obtained for **2a–c** (see Table 1) is on a similar magnitude as the viscosity barrier ( $\sim 1.82$  kcal mol<sup>-1</sup>) in 2-methyltetrahydrofuran (2MTHF), indicating that certain large amplitude motions may couple with the ET process. Both X-ray and AM1 approaches indicate that the phenyl rings are nearly orthogonal to the (2-pyridyl) pyrazolate ligand in **2a–f**, of which the configuration may prohibit the ET process.<sup>‡</sup> It is thus tentatively proposed that in solution phase the ET mechanism may incorporate rotation of the phenyl ring to an optimum orientation so that a through-space ET reaction can take place.

Due to the straightforward syntheses of boron complexes it is feasible to adjust the D/A strength so that the degrees of charge-transfer interactions and consequently the luminescence efficiency can be fine-tuned. An ideal boron-ligands system for devices may exhibit both LE and CT emissions covering an entire white-light region. Work on other systems such as imidazoles and triazoles is currently in progress.

## Notes and references

<sup>‡</sup> CCDC 201833. See <http://www.rsc.org/suppdata/cc/b3/b309374c/> for crystallographic data in .cif or other electronic format.

- (a) Q. Wu, M. Esteghamatian, N.-X. Hu, Z. Popovic, G. Enright, Y. Tao, M. D'Iorio and S. Wang, *Chem. Mater.*, 2000, **12**, 79; (b) Y. Li, Y. Liu, W. Bu, J. Guo and Y. Wang, *Chem. Commun.*, 2000, 1551; Y. Liu, J. Guo, H. Zhang and Y. Wang, *Angew. Chem., Int. Ed.*, 2002, **41**, 182.
- For example, see: (a) T. D. James, K. R. A. S. Sandanayake and S. Shinkai, *Angew. Chem., Int. Ed.*, 1996, **35**, 1910; (b) K. Rurack, M. Kollmannsberger and J. Daub, *Angew. Chem., Int. Ed.*, 2001, **40**, 385; (c) N. DiCesare and J. R. Lakowicz, *J. Phys. Chem.*, 2001, **105**, 6834; (d) W. Yang, H. He and D. G. Drueckhammer, *Angew. Chem., Int. Ed.*, 2001, **40**, 1714; (e) J. Killoran, L. Allen, J. F. Gallagher, W. M. Gallagher and D. F. O'Shea, *Chem. Commun.*, 2002, 1862.
- (a) A. Satake and T. Nakata, *J. Am. Chem. Soc.*, 1998, **120**, 10391; (b) W. R. Thiel and J. Eppinger, *Chem. Eur. J.*, 1997, **3**, 696.
- (a) S.-F. Liu, Q. Wu, H. L. Schmider, H. Aziz, N.-X. Hu, Z. Popovic and S. Wang, *J. Am. Chem. Soc.*, 2000, **122**, 3671; (b) Q. Liu, M. S. Mudadu, H. Schmider, R. Thummel, Y. Tao and S. Wang, *Organometallics*, 2002, **21**, 4743.
- For example, see: (a) U. Mitschke and P. Bauerle, *J. Mater. Chem.*, 2000, **10**, 1471; (b) A. J. Campbell, D. D. C. Bradley, T. Virgili, D. G. Lidzey and H. Antoniadis, *Appl. Phys. Lett.*, 2001, **79**, 3872.
- $k_{\text{et}}$  was deduced by  $k_{\text{obs}} - k_{\text{nr}}$ . The  $k_{\text{obs}}$  value for **2f** was taken as  $k_{\text{nr}}$  due to its non-ET process. Note  $\ln k_{\text{et}} T^{1/2}$  vs.  $1/T$  is also sufficiently linear mainly due to the much larger  $k_{\text{et}}$  value.